Title
Fuel flexibility study of an integrated 25kW SOFC reformer system

Journal
Journal of Power Sources, 144(1)

ISSN
0378-7753

Authors
Yi, Yaofan
Rao, Ashok D
Brouwer, Jacob
et al.

Publication Date
2005-06-01

DOI
10.1016/j.jpowsour.2004.11.068

Available online at www.sciencedirect.com
SCIENCE DIRECT®
Journal of Power Sources 144 (2005) 67–76
JOURNAL OF POWER SOURCES
www.elsevier.com/locate/jpowsour

Fuel flexibility study of an integrated 25 kW SOFC reformer system☆

Yaofan Yi, Ashok D. Rao, Jacob Brouwer, G. Scott Samuelsen *

National Fuel Cell Research Center (NFCRC), University of California, Irvine, CA 92697-3550, USA

Received 4 November 2004; accepted 29 November 2004
Available online 13 April 2005

Abstract

The operation of solid oxide fuel cells on various fuels, such as natural gas, biogas and gases derived from biomass or coal gasification and distillate fuel reforming has been an active area of SOFC research in recent years. In this study, we develop a theoretical understanding and thermodynamic simulation capability for investigation of an integrated SOFC reformer system operating on various fuels. The theoretical understanding and simulation results suggest that significant thermal management challenges may result from the use of different types of fuels in the same integrated fuel cell reformer system. Syngas derived from coal is simulated according to specifications from high-temperature entrained bed coal gasifiers. Diesel syngas is approximated from data obtained in a previous NFCRC study of JP-8 and diesel operation of the integrated 25 kW SOFC reformer system. The syngas streams consist of mixtures of hydrogen, carbon monoxide, carbon dioxide, methane and nitrogen. Although the SOFC can tolerate a wide variety in fuel composition, the current analyses suggest that performance of integrated SOFC reformer systems may require significant operating condition changes and/or system design changes in order to operate well on this variety of fuels.

Keywords: SOFC; Fuel flexibility; Carbon deposition; Syngas; Thermal management

1. Introduction

High-temperature fuel cells (e.g. SOFC and MCFC) have more fuel flexibility than low-temperature fuel cells because carbon monoxide can poison low-temperature electrocatalysts, whereas it works as a fuel in a high-temperature fuel cell [1]. As a result, various fuels can be processed to produce a reformate (containing primarily hydrogen and CO) for direct use in a solid oxide fuel cell. The main fuel sources used to produce this reformate include fossil fuels (e.g. natural gas, oil and coal), and renewable fuels (e.g. biomass and waste). Nuclear power and renewable energy (e.g. solar, wind, wave and hydro) can also be used to produce fuel cell fuels (e.g. by generating electricity and then, H_2 via electrolysis), but these are not considered in this paper. Various fuel processing technologies can be used for any particular fuel source to convert the original fuel to a fuel gas that can be directly used in fuel cells. All fuel processing schemes generate CO, and removal of the CO to levels required by low-temperate fuel cells, such as the PEMFC requires several complex processing steps (e.g. water-gas-shift reaction followed by pressure swing absorption or selective oxidization of the CO) [1].

Although the fuel flexibility advantages of an SOFC have been widely recognized, little experimental data have been published, especially for coal-derived syngas-fueled SOFC systems. Several groups have studied SOFC fuel flexibility in recent years using theoretical analysis or simulation work [2–6]. Marsano et al. [2] found that thermal management of the SOFC stack may be a challenge when operating on disparate fuel sources. In the current study, we focus on thermodynamic issues and constraints that affect the performance of integrated SOFC reformer systems. Thermodynamic system simulation is complemented and supported by experimental investigation of a variety of fuel compositions using an integrated Siemens Westinghouse 25 kW tubular solid oxide

☆ This paper was presented at the 2004 Fuel Cell Seminar San Antonio, TX, USA.

* Corresponding author. Tel.: +1 949 824 5468; fax: +1 949 824 7423.
E-mail address: gss@nfcrc.uci.edu (G.S. Samuelsen).

0378-7753/$ – see front matter © 2005 Elsevier B.V. All rights reserved.
doi:10.1016/j.jpowsour.2004.11.068

Table 1
Baseline compositions and heating values for various fuel sources

Syngas component	Composition (vol.%)			
	NFCRC PNG	Diesel reformate [8]	Biogas [9]	Coal syngas [10]
CO	–	–	–	46
H_2	–	30	–	36
CO_2	1.4	20	40	18
N_2	0.39	–	–	–
CH_4	96.36	50	60	–
C_2H_6	1.45	–	–	–
C_3H_8	0.26	–	–	–
Others	0.14	–	–	–
LHV (kJ mol^{-1})	799.76	474.05	481.77	217.24

fuel cell reformer [7]. The fuel sources included in this study are NFCRC pipeline natural gas (PNG), diesel reformate (after pre-reformer), biogas (e.g. digester gas, landfill gas) and coal-derived syngas. Thermodynamic simulation of the integrated 25 kW SOFC reformer system operating on each of these fuels is followed by experimental tests of selected fuels in the 25 kW SOFC system. The baseline compositions used in the current study are presented in Table 1 and have been determined based on data from the literature [8–10].

2. Twenty-five kilowatt SOFC system description

The Siemens Westinghouse 25 kW tubular solid oxide fuel cell is the first integrated SOFC pre-commercial prototype and research platform. The system was initially installed at the Highgrove Generating Station of Southern California Edison in California in the spring of 1994, and was shipped to the National Fuel Cell Research Center and restarted in January of 1998 [7,11]. As of 2004, the system has operated for a total of 19,750 h with 13,250 h on the current stack (6500 h on its first stack).

The Siemens Westinghouse SOFC is a tubular design configured as a single cell per tube. The system includes 576 tubular cells, each with an inside diameter of 1.18 cm and a length of 50 cm. The tubes are arranged into many sub-groups to aid in the interconnections that make up the fuel cell stack electrical network. The smallest sub-group is a bundle, which contains 18 cells grouped three in parallel, six in series. The next larger size group is a string, which is simply two bundles connected in series. The largest group is a quadrant, made up of four strings. Finally, the four quadrants make up the entire fuel cell stack. The quadrants are isolated from each other such that the performance of one quadrant does not affect the performance of another (other than by radiated heat) [11].

Fig. 1 presents an overall system schematic and details of the SOFC stack design based on natural gas fuel. Compressed and desulfurized natural gas is fed through a mass flow controller to an ejector (also known as a jet pump). The ejector creates a partial vacuum that pulls spent fuel from an anode off-gas recirculation plenum near the top of the stack. This captures water vapor and heat needed for the reforming of natural gas. This fuel mixture passes over nickel-based reformers where methane or any higher hydrocarbons are converted to hydrogen, carbon monoxide, carbon dioxide, and remaining methane. This reformed fuel mixture then enters a fuel manifold at the bottom of the stack where it is distributed to the outside surface of the tubular cells in each quadrant, flowing upwards. Meanwhile, after preheating in a recuperator, air enters the module and passes through the air manifold into air feed tubes that direct air to the bottom inside surface of the tubular cells. Exiting the feed tube, the air flows upward along the inside surface of the tubular cells. With fuel on the outside and oxygen from the air on the inside electro-

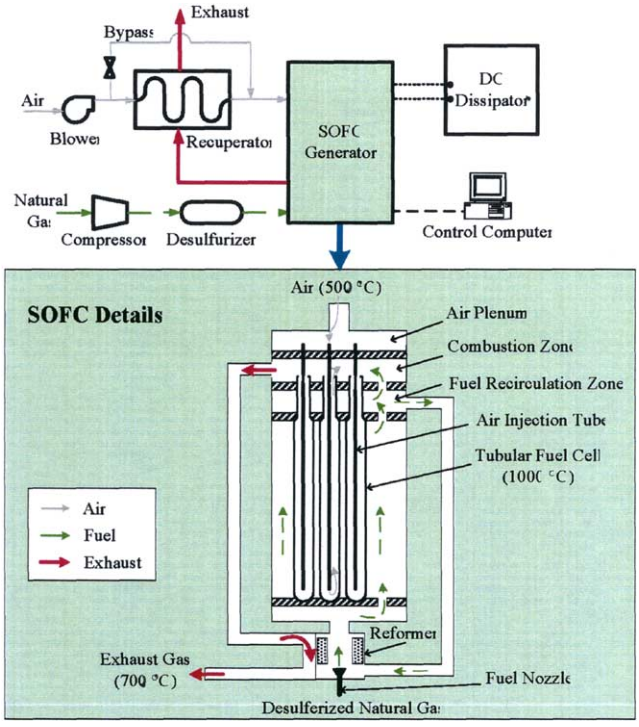

Fig. 1. System schematic and SOFC module details of the Siemens Westinghouse 25 kW SOFC system.

chemical reactions take place along the length of the cells. The temperature inside the module and along the length of each cell varies somewhat, but the maximum temperature is generally kept below 980–1050 °C.

Anode off-gas enters the recirculation plenum where a fraction of it is recirculated and the balance flows into the combustion plenum to mix with the depleted air. The small amount of remaining anode off-gas is combusted with the depleted air to preheat the air through the recuperator and provide heat to the reformers before it is exhausted.

The fuel cell electrical output is connected to a controllable load dissipater that can draw various electrical loads from the fuel cell.

3. Simulation work

3.1. Introduction and validation of simulation tool

The thermodynamic performance of this 25 kW SOFC system was investigated using a state-of-the-art simulation package – Advanced Power Systems Analysis Tools (APSAT) – developed by the Advanced Power and Energy Program at the University of California, Irvine in 2000 [12]. The simulation tool provides modules for modeling traditional and advanced components (compressor, turbine, tubular SOFC, heat exchanger, etc.) for these types of power systems, and users can select the components they need and put them together in various configurations to simulate power plants. The APSAT model has been validated by comparison to 220 kW SOFC and gas turbine hybrid data with high precision (less than 3% error) in previous studies [13].

The APSAT model can well predict the 25 kW SOFC system performance, as shown in the *V–I* curve comparison of Fig. 2. The voltage error between model results and data is lower than 2.7% within the load range of 82–116%. When at nominal load conditions (100% load, or 20 kW DC load from SOFC), the voltage error is only 0.67%.

Table 2
Operating and system parameters for natural gas operation of the integrated 25 kW SOFC system

System parameter	Observed
Natural gas fuel flow (kg s^{-1})	0.82
Compressor air flow (kg s^{-1})	72.2
Fuel compressor drive efficiency (%)	70
Fuel compressor isentropic efficiency (%)	52
Fuel compressor pressure ratio	2.7
Air blower drive efficiency (%)	72
Air blower isentropic efficiency (%)	53
Air blower pressure ratio	1.18
Fuel cell number (cells)	576
Fuel cell length (cm)	50
Fuel cell inside diameter (cm)	1.18
SOFC fuel utilization (%)	82
Anode recirculation ratio (%)	55
Stack temperature (°C)	950
SOFC stoichiometric ratio	6.5
Recuperator heat duty (kJ s^{-1})	42
Recuperator effectiveness (%)	82
Inverter efficiency (%)	90
Heat loss allowance (kW)	10.85
SOFC module	7.3
Heaters	0.55
Ducts	2
Recuperator	1
SOFC air side	5.3
Heaters	0.9
Ducts	2
Recuperator	3.4

A comparison between model results and data acquired using the integrated 25 kW SOFC system is conducted to further validate the model. The parameters applied to the model are set to replicate those observed when acquiring the data as shown in Table 2. Those parameters include inlet streams (fuel and air) data, fuel cell geometry, fuel cell performance settings, settings for balance of plant components, heat losses and pressure losses.

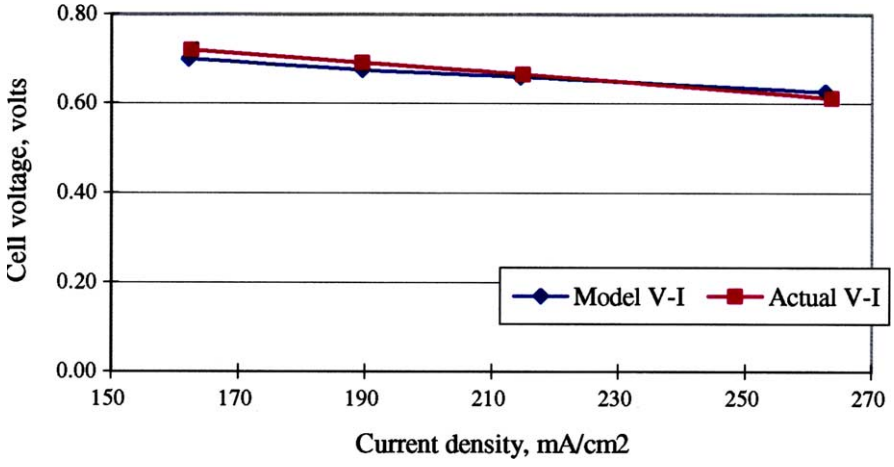

Fig. 2. *V–I* curve comparison between updated model results and actual data (2000).

Table 3
Comparison of system performance: simulation vs. observed

System parameter	Observed	Simulation	Error (%)
SOFC DC power (kW)	20.64	20.28	1.7
SOFC module voltage (volts)	130	127	2.3
Fuel compressor power consumption (kW)	0.34	0.34	0
Air blower power consumption (kW)	2.18	2.20	0.9
Other AC parasitic power (kW)	1.87	1.87	Kept same
DC equivalent system power consumption (kW)	4.87	4.9	0.6
Net system DC power (kW)	15.77	15.38	2.5
SOFC module efficiency (DC/LHV) (%)	52.44	51.48	1.8
Net system efficiency (net AC/LHV) (%)	36.36	35.45	2.5

Major simulation results are compared to data from the 25 kW SOFC system for the operating conditions established in Table 2 are presented in Table 3. For all of the major system performance parameters, the error between experiment and model results is less than 3%.

Fig. 3 presents the system performance at various state points with comparison between simulation results and data for the conditions of Table 2. For every state point, the three critical thermodynamic parameters (temperature, pressure and mass flow rate) are listed and compared. Note that the model states well compare to the observed states of Fig. 3.

The comparisons presented in Table 3 and Fig. 3 indicate that the APSAT model can well simulate the performance of the 25 kW SOFC system and portend significant capability to simulate similar systems and cycles.

3.2. Steady-state simulation

The APSAT SOFC simulation tool demonstrated above was applied to simulate the 25 kW system operating on different fuel sources. To ensure that results for operation with various fuel sources are comparable, all the major system-operating parameters are held constant for each case (see Table 4). Particularly, the air inlet flow rate and stoichiometric ratio are kept the same. Notice that the maximum air flow rate is 84.0 g s^{-1} at an ambient temperature of 17 °C, which is the current limit of the system by blower. Heat losses and pressure losses at different system points are held constant at the values presented in Table 2, which are reasonable approximations for the actual system operation. The fuel mass flow rate is much lower than the air mass flow rate (even for the coal syngas case), which makes the effect of fuel source

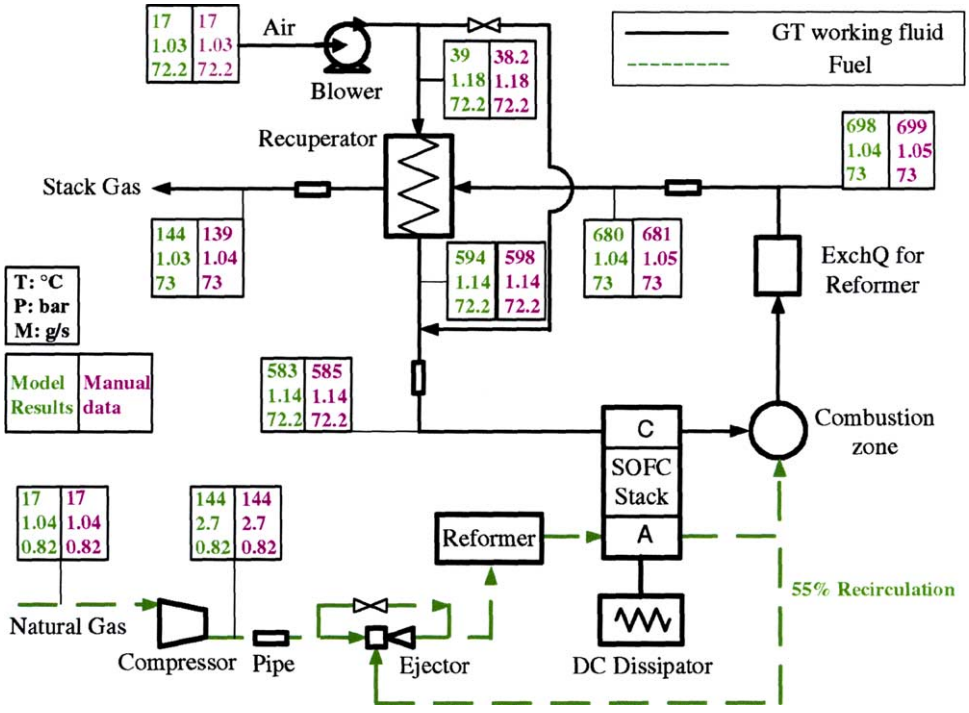

Fig. 3. State points comparison between model results and observed data.

Table 4
System design point operating parameters for various fuel sources

System parameter	Natural gas	Diesel reformate	Biogas	Coal syngas
Fuel flow rate ($g\,s^{-1}$)	0.842	1.515	2.268	4.855
CH_4 content in the fuel (%)	96	50	60	0
Fuel energy (LHV) ($kJ\,s^{-1}$)	40.10	41.17	40.08	51.35
Blower air flow ($g\,s^{-1}$)	73.3	73.3	73.3	73.3
SOFC air inlet ($g\,s^{-1}$)	73.0	73.0	73.0	73.0
SOFC stoichiometric ratio	6.5	6.5	6.5	6.5
SOFC stack temperature (°C)	950	950	950	950
Overall fuel utilization (%)	82	82	82	82
Fuel utilization per passage (%)	73.2	76.1	76.1	79.5
Recirculation ratio (%)	40	30	30	15
Reformer inlet C—H—O content (%)				
C	16	16	21	28
H	63	61	50	34
O	21	23	29	38
Recuperator heat duty ($kJ\,s^{-1}$)	42.75	42.75	42.75	36.82

variation on the overall system heat losses and pressure losses quite insignificant.

In the current model work, fuel compression is ignored since the natural gas case can use pipeline gas pressure that is sufficient (greater than 5 bar) and the syngases can assume to be compressed before delivery to the system to sufficient pressure.

Overall fuel utilization is held constant (82%) for each of the cases simulating operation with various fuels as shown in Table 4. Anode off-gas recirculation ratios for the different fuel sources are varied based on their heating values. The design basis for setting the recirculation ratio is explained in a later section of this paper. The recirculation ratios depend upon the fuel source as shown in Table 4. These recirculation ratios are designed to be high enough to avoid carbon deposition based on chemical equilibrium calculations. As can be seen, the recirculation ratio decreases with the heating value of the fuel. For the medium BTU fuels (diesel reformate and biogas), the recirculation ratio is 75% of that for natural gas while for the low BTU fuel (coal syngas) it is less than 40% of that for natural gas.

The overall simulated performance comparison for operation of the integrated SOFC reformer system on the various fuel sources is presented in Table 5 and Fig. 4. The SOFC system performance does not change significantly when the fuel is switched from natural gas to diesel reformate or biogas. However, the system performance changes significantly when fuel is switched to coal-derived syngas. The net system efficiency when operating on diesel reformate or biogas is slightly lower than the natural gas case. When operating on coal syngas, net system efficiency is about 10 percentage points lower than the natural gas case due to the high, unrecovered heat contained in the system exhaust. The voltages (cell and module) and system DC power output when operating on diesel reformate, or biogas, are close to those of the natural gas case. When operating on coal gas, voltages and power are lower than the natural gas case due to the significant fuel dilution effect.

In Fig. 5, the major thermodynamic parameters (temperature, pressure and mass flow rate) at major state points in the system are compared for different fuel sources. The exhaust temperature of the biogas and diesel reformate cases are, respectively, 7 and 21 °C higher than the natural gas case. These temperatures increase because CH_4 content in diesel reformate and biogas is lower than that in natural gas. It should be noted that the endothermic reformation reaction of CH_4 is helpful in absorbing sensible heat contained in the fuel cell exhaust. Thus as more heat is recovered by the reformation process, the exhaust temperature and heat wasted to the environment are lowered. However, these temperature increases are not likely to significantly challenge the equipment design limits for these cases investigated herein.

The exhaust temperature of the coal-derived syngas case is 153 °C higher than natural gas case as shown in Fig. 2. This high exhaust temperature is due to the lack of a chemical heat sink (endothermic CH_4 reformation chemistry) in the SOFC system. The CH_4 content in the coal gas is nearly zero, while the CO content is high and the CO shift reaction is exothermic. Therefore, compared to the natural gas case, more heat is generated in the SOFC stack while no heat is recovered by downstream reformation. When an SOFC is coupled with a

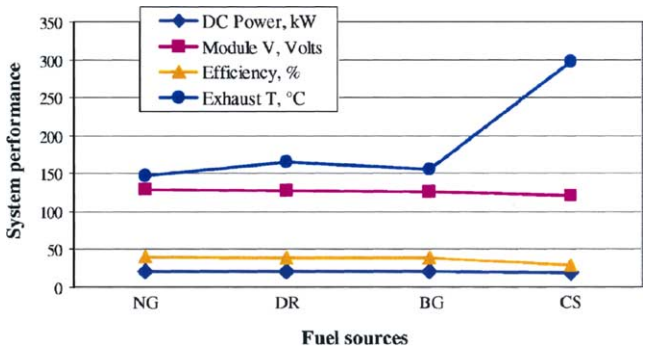

Fig. 4. Design performance comparison for various fuel sources (NG: natural gas; DR: diesel reformate; BG: biogas; CS: coal syngas).

Table 5
Design performance comparison of the integrated SOFC system operating on various fuel sources

System parameters	Natural gas	Diesel reformate	Biogas	Coal syngas
SOFC DC power (kW)	21.12	20.94	20.64	19.70
Cell voltage (volts)	0.668	0.662	0.653	0.632
Module voltage (volts)	128.4	127.0	125.3	121.3
Air blower power consumption (kW)	2.23	2.23	2.23	2.23
Other AC parasitic power (kW)	1.87	1.87	1.87	1.87
SOFC module efficiency (DC/LHV) (%)	52.7	50.9	51.5	38.4
System efficiency (net AC/LHV) (%)	37.2	35.8	36.1	26.5
System exhaust temperature (°C)	148	166	155	298

gas turbine or other bottoming cycle for electricity generation and/or heat recovery, it is expected that the exhaust heat loss of the coal derived syngas case can be significantly reduced, leading to higher system efficiencies.

3.3. Anode off-gas recirculation analysis

3.3.1. Anode recirculation versus carbon deposition

When operating the SOFC system with carbon containing fuel (hydrocarbon, CO, etc.), one must avoid carbon deposition within the fuel cell stack, internal and external reformer, and other system components. Two strategies can be applied:

(1) Increase the operating temperature wherever fuel is present, so that the chemical equilibrium moves away from the region in which carbon formation and deposition occur.
(2) Maintain high moisture content in the fuel, which increases H and O content of the fuel stream shifting the chemical equilibrium and kinetics to regimes that do not favor carbon formation and deposition.

For the case of the 25 kW SOFC system, the normal minimum operating temperature in the fuel cell stack is about 850 °C. The operating temperature of the internal reformer is about 750 °C, which is maintained by a combination of heat transferred from the fuel cell exhaust and anode off-gas recycle as shown in Fig. 1. The anode off-gas recirculation provides heat as well as moisture to the fuel gas to aid the reforming reactions and to prevent carbon deposition in the reformer. This is accomplished by a fuel ejector pump that produces a low pressure to recirculate a fraction of the anode off-gas, which has a higher O/C ratio than the fresh fuel and significant water content. For a given pressure of the fresh fuel, the recirculation ratio can be manually adjusted by varying the fraction of fresh fuel flow rate that passes through the ejector and a fuel by-pass valve as shown in Figs. 3 and 5. Thus, for a given fresh fuel bypass flow, the current 25 kW SOFC control strategy does not allow an independent change of reformer operating temperature according to the moisture content to obtain best reforming performance. Instead, it seeks to maintain constant reformer operating temperature.

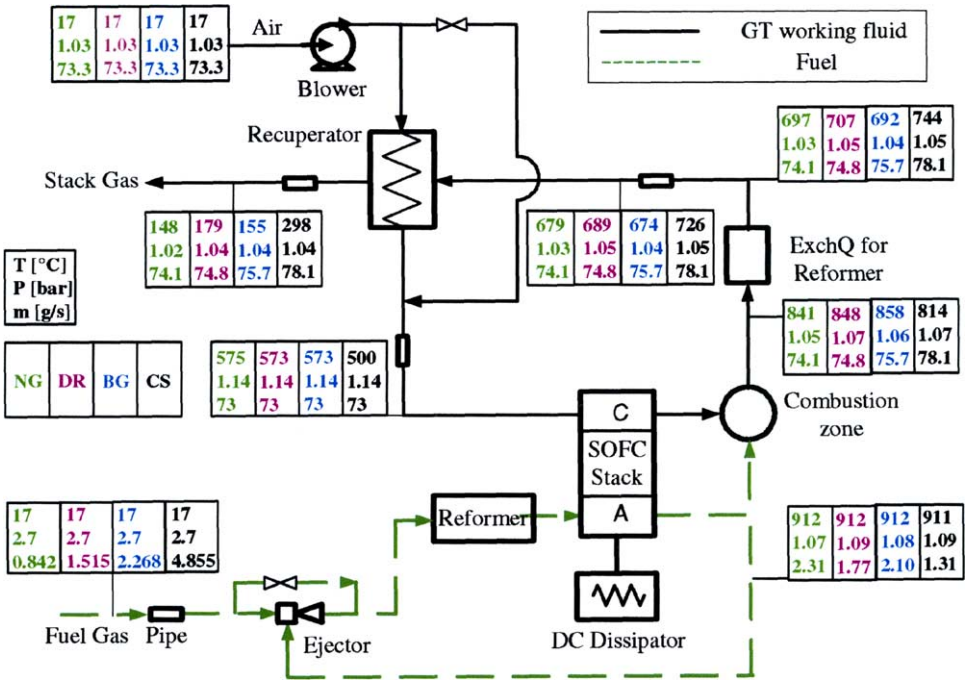

Fig. 5. Comparison of design state points for various fuel sources.

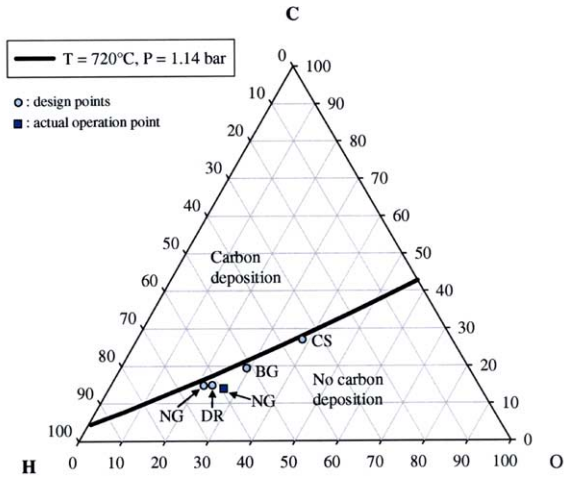

Fig. 6. C–H–O ternary diagram.

The following issues must be considered when determining an appropriate anode off-gas recirculation ratio:

(1) *The recirculated anode off-gas should provide sufficient moisture for the methane reformation or CO shift reaction and avoid carbon deposition.* The NASA chemical equilibrium code [14] is applied to determine the carbon deposition for the cases of interest in this study. The criteria used to determine, whether or not carbon is formed at equilibrium is 1 ppm of solid carbon. The carbon deposition line that results from these equilibrium computations for conditions of 720 °C and 1.14 bar is presented in the C–H–O ternary diagram of Fig. 6. This line corresponds to the equilibrium conditions that could possibly lead to carbon deposition (graphite or amorphous). Note that actual carbon formation and deposition is often controlled by kinetic phenomena (chemistry, mass transport, . . .), but is only favored (driven by chemical equilibrium) above the line presented in Fig. 6. Thus, one should design a system to operate under average conditions that are significantly below the line. The design points selected as a result of this analysis are shown in Fig. 6 for the different fuel cases. Note also that the temperature condition of Fig. 6 (720 °C) is 30 °C lower than the average reformer operating temperature. Each design point is significantly below the carbon formation line. Since the operating temperature in the SOFC stack is higher than that in the reformer, carbon deposition should not occur within the SOFC stack.

(2) *The recirculation ratio should be achievable with the existing ejector.* Based on the ejector performance observed during system operation and considering the overall ejector control strategy, it is expected that the design recirculation ratios required to meet the conditions represented in Fig. 6 are feasible for each of the fuel streams of interest. An ejector CFD model will be built in the future and applied to simulate the performance to confirm that the designed recirculation ratios can be achieved.

(3) *The selected recirculation ratio can help improve the overall system performance.* The effect of varying the recirculation ratio on system efficiency as simulated by the APSAT code is shown for the different fuel source cases in Fig. 7. These results are presented along with the selected design point (black ovals) for each of the fuel sources where system efficiency is maximized while avoiding carbon deposition.

(4) *The design recirculation ratio is dependent on the fresh fuel composition.* Fig. 7 shows that the minimum recirculation ratio to avoid carbon deposition is different for each of the fuel sources. As shown in the figure, carbon (graphite and amorphous) can potentially form in the area left of the dashed line, while on the right of dashed line, the recirculation ratio is high enough to provide sufficient moisture to avoid carbon deposition. At the design pressure (1.14 bar) and temperature (720 °C), natural gas fuel needs the highest minimum recirculation ratio (−38%), while coal syngas requires the smallest ratio (∼14%). Since for coal syngas, the O content is highest among all the fuel cases, the recirculation ratio for coal syngas that is required to avoid carbon deposition is the lowest, while the recirculation ratio required for natural gas is the highest due to its low O content.

3.3.2. Anode recirculation versus SOFC system performance

The effect of changing the fuel recirculation ratio on the SOFC system efficiency is interesting. When the overall fuel utilization is held constant, an increase in the recirculation ratio affects the fuel cell system performance primarily in two ways:

(1) Fuel is diluted by the moisture and CO_2 contained in the recirculated anode off-gas. The dilution effect causes a decrease in the Nernst potential.

(2) The fuel utilization per passage, which is a function of overall fuel utilization and anode off-gas recirculation ratio, as shown below, is reduced.

$$U_{f,p} = \frac{U_f(1-R)}{1-U_f R} \quad (1)$$

where $U_{f,p}$ is the fuel utilization per passage, U_f the overall fuel utilization, and R the anode off-gas recirculation ratio. The decrease in fuel utilization per passage can help reduce concentration polarization and lead to lower "effective fuel utilization."

The dilution effect is more significant than the fuel utilization effect when fuel utilization per passage is not too high. But when fuel utilization per passage is high while the recirculation ratio is low, the fuel utilization effect becomes more significant. Thus, Fig. 7 shows that maximum system efficiency can be achieved when the recirculation ratio is set at 40% for natural gas case, and 30, 20, and 15% for cases of diesel reformate, biogas and coal syngas, respectively. To avoid carbon deposition, which can happen at a recirculation

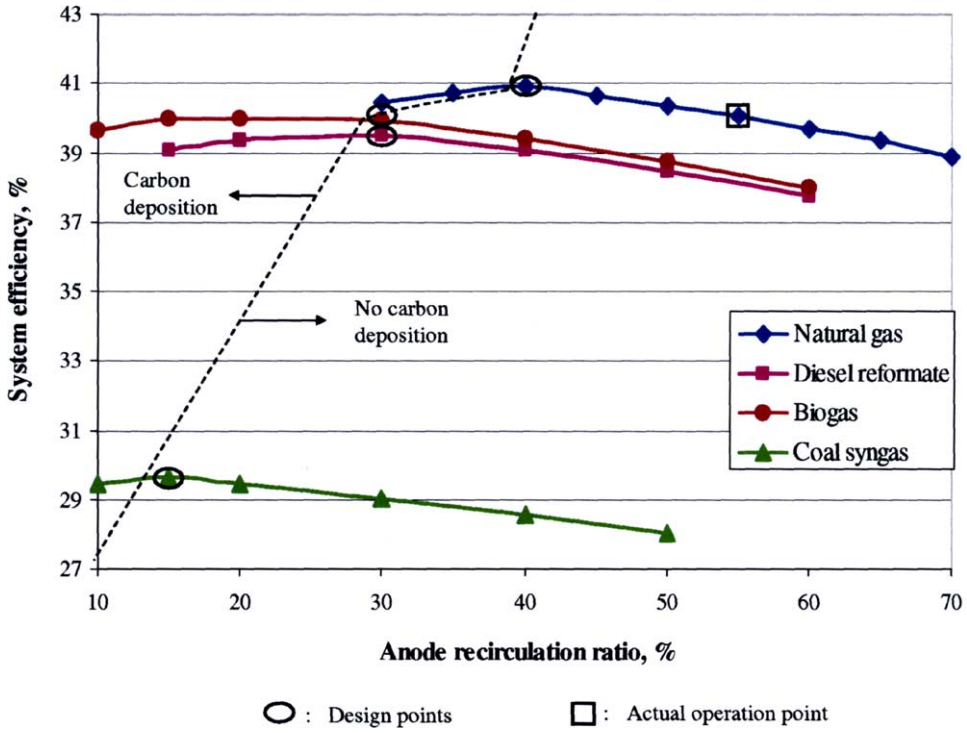

Fig. 7. Effect of anode recirculation ratio on system performance for various fuel sources (overall fuel utilization is held constant at 82%).

ratio of 20% for biogas, the design recirculation ratio has to be increased to 30%. This design point somewhat compromises system efficiency. For the natural gas case, the system efficiency is maximized at a recirculation ratio of 40%. The APSAT simulation of Fig. 7 suggests that operating the system with a 40% recirculation instead of the 55% operating point selected by Siemens Westinghouse can increase system efficiency by 1 percentage point. Lowering the recirculation to 40%, however, increases the risk of carbon deposition. In the case of coal syngas, a decrease in the recirculation ratio from 50 to 15% can contribute to an increase in system efficiency of as much as 2 percentage points.

4. Discussion

Based on the above observations and analyses, potential solid oxide fuel cell system design and operating challenges associated with operation on various fuel sources are discussed. Challenges especially related to coal syngas operation are identified with corresponding strategies suggested to address each challenge.

4.1. Thermal management

Four principle strategies can be applied to control the stack temperature of an integrated SOFC system within a safe operating range. One strategy manipulates the stoichiometric ratio or air flow rate. In most systems however, the maximum air flow rate may be limited, as is the case for the current system due to its air blower capacity. A second strategy manipulates the fuel cell air inlet temperature, which can be controlled by reducing the amount of heat transferred in the recuperator or using an exhaust bypass valve. This strategy also has its limitations since the fuel cell stack cannot tolerate a large temperature gradient that may be introduced at the cathode inlet if air temperature is too low. The third strategy is to manipulate the system load. The operating temperature may be reduced by decreasing the load but at the expense of reduced power output (even though this may not be desired in a practical application it may be necessary to protect the fuel cell). Fourth, one can use varying levels of internal reformation to cool the fuel cell stack (not an option with the current 25 kW system). A combination of these strategies may also be implemented. Each of these control strategies can be automated in the 25 kW SOFC control system.

It is expected that the thermal management for the diesel reformate and biogas cases can be achieved without modification to the current integrated SOFC control system. However, for the coal syngas case, the stack air inlet temperature should be controlled via the recuperator bypass to prevent stack overheating. As a result, the heat transfer rate for the recuperator in the simulated coal syngas case (see Table 4) was set at approximately 6 kJ s^{-1} lower than that used for the other fuel cases, representing a larger recuperator bypass flow.

4.2. Recuperator

The recuperator plays a crucial role in adjusting fuel cell stack temperature. Investigation of recuperator operation for

preventing an unexpected failure of the SOFC system or damage to the recuperator itself is included in this study. Challenges are investigated in two major aspects: temperature and heat transfer rate.

4.2.1. Temperature

The first concern identified by APSAT simulation of the integrated system operated on coal syngas is whether the recuperator materials can withstand operation at temperatures in excess of 730 °C (the simulated recuperator inlet temperature for these conditions). The current experimental recuperator module is made out of stainless steel, and this particular grade of stainless steel can handle temperatures as high as 870 °C. This may not generally be the case for integrated SOFC systems with similar recuperators. When operating on coal gas, the recuperator operating temperature of an integrated SOFC system of this type is a major design concern.

4.2.2. Heat transfer rate

The stack air inlet temperature (recuperator shell outlet temperature) can be controlled in the simulation via a simple adjustment of the recuperator heat transfer rate. This heat transfer rate depends on the following control function:

$$Q = F \times \Delta T_{\text{mean}} \times U \times A = m_{\text{air}} \times C_p \times \Delta T_{\text{cold}} \qquad (2)$$

where factor F is dependent on the recuperator geometric configuration and overall heat transfer coefficient, U, which is dependent on the recuperator inlet and outlet temperatures. To lower or avoid a surge in the heat transfer rate, the log mean temperature difference ΔT_{mean} should be decreased, which can be accomplished by increasing the recuperator by-pass flow rate (or by decreasing the air side mass flow rate). Note that U increases when the recuperator operating temperature increases (e.g. an increase in exhaust side temperature), which causes a further increase in the heat transfer rate, Q.

This analysis suggests that if the air side mass flow rate is kept low enough, then the recuperator heat transfer rate can be controlled to achieve a desired stack inlet temperature. For the current SOFC system, analyses determined that the control of recuperator air side mass flow rate can be fully realized via adjustment of the recuperator by-pass flow rate (see Fig. 1). In addition, the control strategy for the fuel transition from natural gas to coal syngas allows the system to operate on a varying mixture of natural gas and coal gas with an increase of coal gas content that can be adjusted in a stepwise fashion. This strategy helps the SOFC control system to adjust the control parameters to obtain successful operation and maintain safe operating temperature conditions in the SOFC stack.

4.3. Exhaust duct

As shown before for the coal syngas case, the exhaust temperature can be as high as 300 °C. The materials used for the current exhaust duct and fan have the capability to handle such a high temperature in the current unit. However, increased exhaust temperatures that result from coal syngas operation may be of general concern in other applications.

4.4. Air blower capacity challenge

The general concern is to design integrated SOFC systems that can operate on various fuel gases with air blowers that have sufficient capacity flexibility. In particular, higher air blower capacity is required for the syngas cases compared to the case of natural gas operation. For the coal gas case, due to the significant increase in exhaust temperature and recuperator operating temperature, the air inlet temperature to the stack is expected to be higher, and air blower operating temperature may also increase due to the air blower being located in close proximity to the recuperator. Thus, the air blower capability for the current integrated SOFC system may not be sufficient to fully control stack temperature for the coal syngas case. As a result, the design air flow rate (or stoichiometric ratio) is kept lower than the normal air blower capacity limit (see Table 4) for the coal syngas case. If the design air flow rate cannot be reached, the system load may have to be reduced to relieve the stack temperature increase that would otherwise result from the lack of sufficient cooling air for the current integrated SOFC system.

4.5. Ejector

The proper control of the fuel ejector plays an important role in the system operation [15]. Due to the significant change in mass flow rate for the different fuel sources considered in this study, the performance of the fuel ejectors and the corresponding by-pass valves must be understood. For the current 25 kW SOFC control system, we are not confident that one can adjust the ejector flow rate and the corresponding anode off-gas recirculation rate by controlling the ejector by-pass valve with sufficient precision and range. This will be investigated in future experimental studies.

4.6. Fuel compressor

The fuel compressor should be able to provide enough pressure for the ejector to recirculate the required amount of anode off-gas. The fuel compressor compression ratio likely must be varied for different fuel sources and recirculation ratios. The fuel compressor exit pressure and ejector by-pass control can be controlled in a congruent manner to reach all of the different recirculation requirements for the current system. Therefore, when operating the current system on the various fuel types, the fuel compression ratio will be varied as a function of the overall fuel utilization setting, recirculation ratio and fuel flow rate. In the current experimental design work and simulations, the compression ratio is kept the same for the various fuels as a simplification. Nonetheless, the detailed understanding of the coupled and interactive impacts of fuel compressor and ejector performance as a function of

fuel type is important to understand and will be a subject of future work.

5. Summary

The fuel flexibility of a particular integrated 25 kW SOFC reformer system is studied. Strategies for system operation on different fuel sources are designed and evaluated using chemical equilibrium and advanced thermodynamic simulation tools. Generalized discussion of the impacts of multi-fuel operation of integrated SOFC reformer systems on component performance, design point selection, thermal management and overall system efficiency is included. Potential operating challenges are identified and discussed for operation of a particular 25 kW SOFC system and generalized integrated SOFC reformer systems on these types of fuels.

Major conclusions are:

(1) The APSAT model can well simulate the performance of the 25 kW SOFC system and portends significant capability to simulate similar systems and cycles.
(2) Simulation results show that design conditions can be identified that allows the integrated SOFC system to operate on medium BTU fuel gas (e.g. diesel reformate and digester gas) with system performance close to that of natural gas operation.
(3) Operation of the SOFC system on low BTU fuel gas (e.g. coal-derived syngas) is much more challenging, however, leading to lower system efficiency at the design point and significant system thermal management challenges. Strategies to solve the thermal management challenges are discussed and will be tested in the future experimental work.
(4) When an SOFC is coupled with a gas turbine or other bottoming cycle for electricity generation and/or heat recovery, it is expected that the exhaust heat loss of the coal-derived syngas case can be significantly reduced, leading to higher system efficiencies.
(5) A proper design of anode off-gas recirculation ratio can improve SOFC system efficiency and avoid carbon deposition within the reformer and SOFC stack. The optimum recirculation ratio is different for each of the fuel types. It is important to have proper control of fuel flow rate and recirculation ratio to maintain reformer temperature, provide sufficient steam, and avoid carbon deposition.

Acknowledgements

We acknowledge and appreciate the support of Southern California Edison, Siemens Westinghouse Power Corporation, and the California Energy Commission in the preparation of this paper.

References

[1] J. Larminie, A. Dicks, Fuel Cell Systems Explained, second ed., John Wiley and Sons, 2003.
[2] F. Marsano, L. Magistri, M. Bozzolo, O. Tarnowski, Influence of fuel composition on Solid Oxide Fuel Cell hybrid system layout and performance, ASME Turbo Expo GT2004-53853, Vienna, Austria.
[3] K. Eguchi, H. Kojo, T. Takeguchi, R. Kikuchi, K. Sasaki, Fuel flexibility in power generation by solid oxide fuel cells, Solid State Ionics 152–153 (2002) 411–416.
[4] F.A. Coutelieris, S. Douvartzides, P. Tsiakaras, The importance of the fuel choice on the efficiency of a solid oxide fuel cell system, J. Power Sources 123 (2) (2003) 200–205.
[5] S.L. Douvartzides, F.A. Coutelieris, A.K. Demin, P.E. Tsiakaras, Fuel options for solid oxide fuel cells: a thermodynamic analysis, AIChE J. 49 (1) (2003) 248–257.
[6] Fuel Cell Handbook, NETL, U.S. Department of Energy, 2000.
[7] S.C. Singhal, Advances in solid oxide fuel cell technology, Solid State Ionics 135 (2000) 305–313.
[8] SCE/SW former 25 kW SOFC project on logistic fuel study, Southern California Edison/Siemens Westinghouse Power Corporation, 1995.
[9] G. Bush, King County Fuel Cell Demonstration Project, Renton, Washington, 2003.
[10] Wabash River Coal Gasification Repowering Project, Wabash River Energy Ltd., 2000, pp. 4–80.
[11] W.J. Skrivan, Parametric testing and analysis of a 25 kW SOFC system, Master Thesis, Department of Mechanial and Aerospace Engineering, University of California, Irvine, 2002.
[12] A.D. Rao, G.S. Samuelsen, Analysis strategies for tubular SOFC based hybrid systems, ASME J. Eng. Gas Turbines Power 124 (2002).
[13] Y. Yi, T.P. Smith, J. Brouwer, A.D. Rao, G.S. Samuelsen, Simulation of a 220 KW hybrid SOFC gas turbine system and data comparison, Eighth International Symposium on Solid Oxide Fuel Cell (SOFC-VIII), 2002, Paris, France, 2002.
[14] S. Gordon, B.J. McBride, Computer program for calculation of complex chemical equilibrium compositions and applications I. Analysis, National Aeronautics and Space Administration Lewis Research Center, Cleveland, 1994.
[15] F. Marsano, L. Magistri, A.F. Massardo, Ejector performance influence on a solid oxide fuel cell anodic recirculation system, J. Power Sources 129 (2) (2004) 216–228.